13th World Conference on Earthquake Engineering
Vancouver, B.C., Canada
August 1-6, 2004
Paper No. 634

PERFORMANCE OF COLUMN-FOUNDATION SUB-ASSEMBLIES UNDER MONOTONIC LATERAL LOAD

Jaswant N. ARLEKAR[1] and C. V. R. MURTY[2]

SUMMARY

Traditional studies on column bases have generally concentrated on design of concrete pedestal for the columns, column base plates, and the anchorage between the base plates and pedestals. Few studies have been reported on the design of column-to-foundation connections using the capacity design concept. In this paper, 4 types of column-foundation sub-assemblages are analytically studied. The sub-assemblages selected here represent various column-foundation configurations and loadings possible in steel MRF buildings. These column-foundation sub-assemblages are subjected to monotonic lateral displacement under axial load. The nonlinear responses of these sub-assemblages provide valuable insights into their possible earthquake performance, which may be useful in developing seismic design criteria for column base connections.

INTRODUCTION

The current design procedures for the design of column bases is not as developed as the procedures for the design of beam-to-column joints and connections. As per the existing procedures (e.g., AISC, 1990), column base plates and pedestals are designed for the column axial loads from analysis and with small moments. The main emphasis is on the transfer of the column loads, usually pure axial loads with nominal moments, to the foundation. Thus, in most procedures the entire effort is to proportion the column base plate such that there is no stress concentration due to its bearing on the foundation. Further, the shear resistance at the column base (an aspect of column bases that is covered fairly adequately in literature) is provided by the bearing of the anchor bolts against the concrete pedestal. A summary of the existing status of the column base procedures design is presented elsewhere (Arlekar, 2002).

The combined presence of axial force (P), shear force (V) and bending moment (M) at a column-to-foundation connection (during strong earthquakes) makes its design unique and significantly different from that of a beam-to-column connection. Four types of sub-assemblages are studied in this paper; these are designed using a capacity design procedure developed to consider the combined effect of P, V and M (Arlekar and Murty, 2002).

[1] Ph.D., Gawmwaddi, Anjuna, Bardez, Goa 403509, India, Email: jaswant_arlekar@hotmail.com
[2] Professor, Department of Civil Engineering, IIT Kanpur, India, Email: cvrm@iitk.ac.in

PERFORMANCE OF COLUMN-TO-FOUNDATION JOINTS IN PAST EARTHQUAKES

Prior to the 1994 Northridge earthquake, no damages to column-to-foundation joints in steel moments resisting frames (MRFs) have been reported. This is not surprising as very few steel structures have been subjected to strong earthquake shaking prior to the 1994 Northridge event. A few damages to steel column bases were reported after the 1994 Northridge earthquake. Buildings that sustained damages to column bases during this earthquake had a typical configuration; the columns were welded to the base plate, and the base plate was anchored to the concrete pedestal with four anchor bolts. Failure to such column bases includes (a) fractures in the base plate extending through its thickness and across its width, (b) pull out of anchor bolts, and (c) horizontal cracks along the welds connecting column flanges to base plate (Figure 1) (Krawinkler, et al., 1996). Crushing of the concrete pedestal suggested substantial vertical impact of the base plate against concrete (Bertero, et al., 1994). A year later, during the 1995 Kobe earthquake, column-to-foundation connection sustained extensive damage in the form crushing of concrete pedestal (Figure 2a), pull-out of anchor bolts (Figure 2b), uplift of base plate, and cracking of the welds at the column base (AIJ, 1995).

The 1994 Northridge and 1995 Kobe earthquakes are two events that have effectively highlighted the vulnerability of welded steel MRFs during earthquakes. Although substantial research has been conducted to improve the design of beam-to-column connections, the design of column-to-foundation connections in steel welded MRFs to resist earthquakes is still in the nascent stage, and needs to be developed considerably.

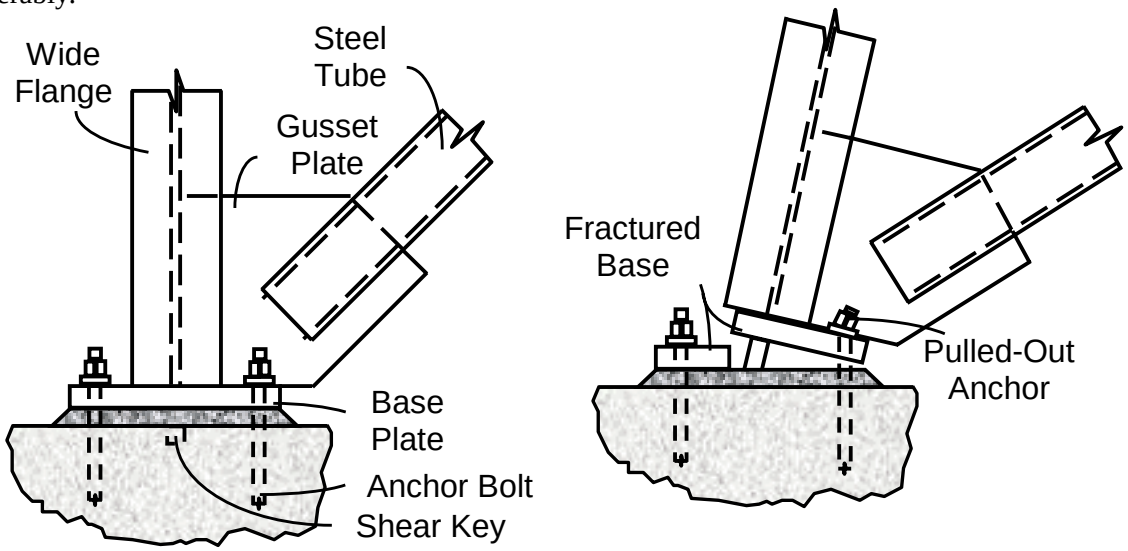

Figure 1: Column foundation failure: Schematic representation of column-foundation joint of the 4-storey Oviatt Library building at the California State University, Northridge, (a) before, and (b) after the 1994 Northridge earthquake, showing anchor bolt pull-out due to fracturing of base plate (Krawinkler, et al., 1996). Base-plate fracture and consequent base plate rotation resulted in significant drifts in upper storeys of the building.

(a) (b)

Figure 2: Column foundation damage: (a) Crushing of concrete pedestal of column-foundation joint due to pounding of base plate on the pedestal, and (b) Pull-out of anchor bolts and crushing of concrete pedestal at column-foundation joint during 1995 Kobe earthquake (AIJ, 1995). Pounding of base plate and pull-out of anchor bolts implies significant uplift of the base plate.

NUMERICAL STUDY – PUSHOVER ANALYSIS

The four types of columns, namely, (a) interior column of a MRF with light gravity loads, (b) interior column of a MRF with heavy gravity loads, (c) exterior column on the compression (leeward) side of a frame, and (d) exterior column on the tension (windward) side of a frame, are subjected to nonlinear pushover analyses to assess their capacity to sustain large, and to study the performance of the connection elements, which are designed using the capacity design procedure developed by the authors (Arlekar and Murty, 2002).

The geometry, loading and support conditions of the subassemblages are shown in Figure 3. The details the column-to-foundation connections concrete pedestals are listed in Table 1. A36 grade of steel (F_y = 250 MPa) is used for both column and the connection elements. M30 (f_{ck} = 30 MPa) concrete is for the pedestal. The flange cover plates and vertical rib plates are designed assuming that the smallest compressive axial load in the column $0.2P_y$. The base plate and concrete pedestal are designed as per Manual of Steel Construction (AISC, 1989) for an axial force equal to the yield capacity P_y of column. Four 32 mm diameter bolts are provided to anchor the base plate with the concrete pedestal.

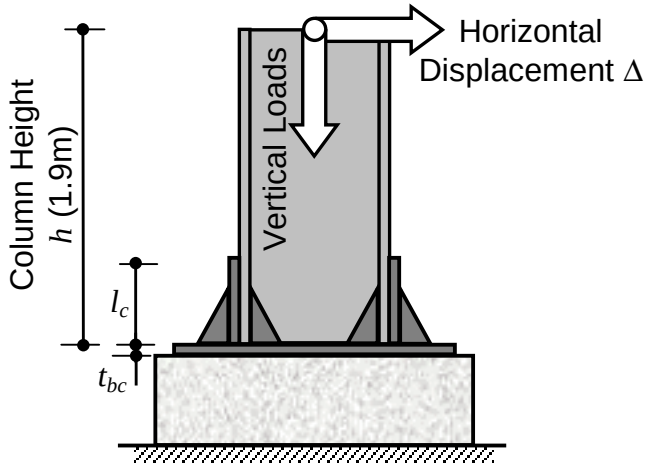

Figure 3: Geometry, loading and boundary conditions for the subassemblages analyzed.

In the finite element models, the concrete of pedestal is modeled using the FAIL STRESS option of ABAQUS software (HKS, 1998), with compressive failure stress of 30 MPa, and shear failure stress of 2.25 MPa. The bottom nodes of the concrete pedestal are completely restrained. The steel column and concrete pedestal are modeled using 8-noded solid elements, with finer mesh near the connection. Figure 4 shows details of the finite element discretisation for a typical column base (W14×455). Base plate uplift is not modeled. *Y*-symmetric boundary conditions are applied at the nodes on the vertical plane passing through the column web at its mid-thickness, to reduce the finite element model size to a half.

Table 1: Dimensions of connection element plates and concrete pedestal.

Column Section	***Dimensions*** (mm)											
	Cover Plate			***Rib Plate***			***Base Plate***			***Pedestal***		
	h	*w*	*t*	*h*	*w*	*t*	*l*	*w*	*t*	*l*	*w*	*h*
W36×300	255	340	45	255	275	45	1170	640	95	2020	1110	485
W27×178	220	300	30	85	135	30	1100	570	65	1600	830	285
W21×147	190	260	30	145	100	30	820	540	65	1300	850	250
W16×100	160	215	25	110	70	25	700	500	55	1020	730	160
W14×730	1165	555	125	410	110	125	1220	1120	230	2435	2235	610
W14×455	680	600	85	290	110	85	980	870	180	1955	1735	500
W14×257	225	305	50	45	70	50	730	665	115	1450	1320	360
W14×176	240	330	35	20	70	35	640	610	80	1175	1120	270
W14×61	155	210	20	85	55	20	615	485	30	760	600	75
W12×336	440	330	60	145	95	50	860	730	160	1720	1460	365
W12×210	165	225	50	140	100	30	675	585	115	1345	1165	335
W10×112	145	200	32	65	40	32	555	495	75	970	865	210

Loading for Pushover Analysis

The connection subassemblages are subjected to the following four types of pushover loadings. These are discussed below.

Case (a): (0.2Py) Plus Pushover of (200mm)

Step 1: Apply gravity compressive force P of $0.2P_y$ on the column

Step 2: Apply monotonic horizontal displacement Δ of 200mm at the free end of column, in increments

Case (b): (0.5Py) Plus Pushover of (200mm)

Step 1: Apply gravity compressive force P of $0.5P_y$ on the column

Step 2: Apply monotonic horizontal displacement Δ of 200mm at the end of column, in increments

Case (c): (0.5Py) Plus Pushover of (0.5Py and 200mm)

Step 1: Apply gravity compressive force P of $0.5P_y$ on the column

Step 2: Apply additional monotonic compressive axial load of $0.5P_y$ and monotonic horizontal displacement Δ of 200mm at the free end of column, in increments

Case (d): (0.5Py) Plus Pushover of (-0.4Py and 200mm)

Step 1: Apply gravity compressive force P of $0.5P_y$ on the column

Step 2: Apply additional monotonic tensile axial force of $-0.4P_y$ and monotonic horizontal displacement of 200mm at the free end of column, in increments

The column in case (a) is lightly loaded with initial gravity load of $0.2P_y$ and subjected to a large lateral displacement; it represents an interior column of a MRF with light gravity loads. The column in case (b) is heavily loaded with initial gravity load of $0.5P_y$ and subjected to a large lateral displacement; it represents an interior column of a MRF with heavy gravity loads. The column in case (c) is again heavily loaded column with initial gravity load of $0.5P_y$ and subjected to a large lateral displacement simultaneously with

an increase in axial compression; it represents an exterior column on the compression (leeward) side of a frame. Similarly, the column in case (d) is heavily loaded with initial gravity load of $0.5P_y$ and subjected to large lateral displacement simultaneously with a decrease in axial compression; it represents an exterior column on the tension (windward) side of a frame.

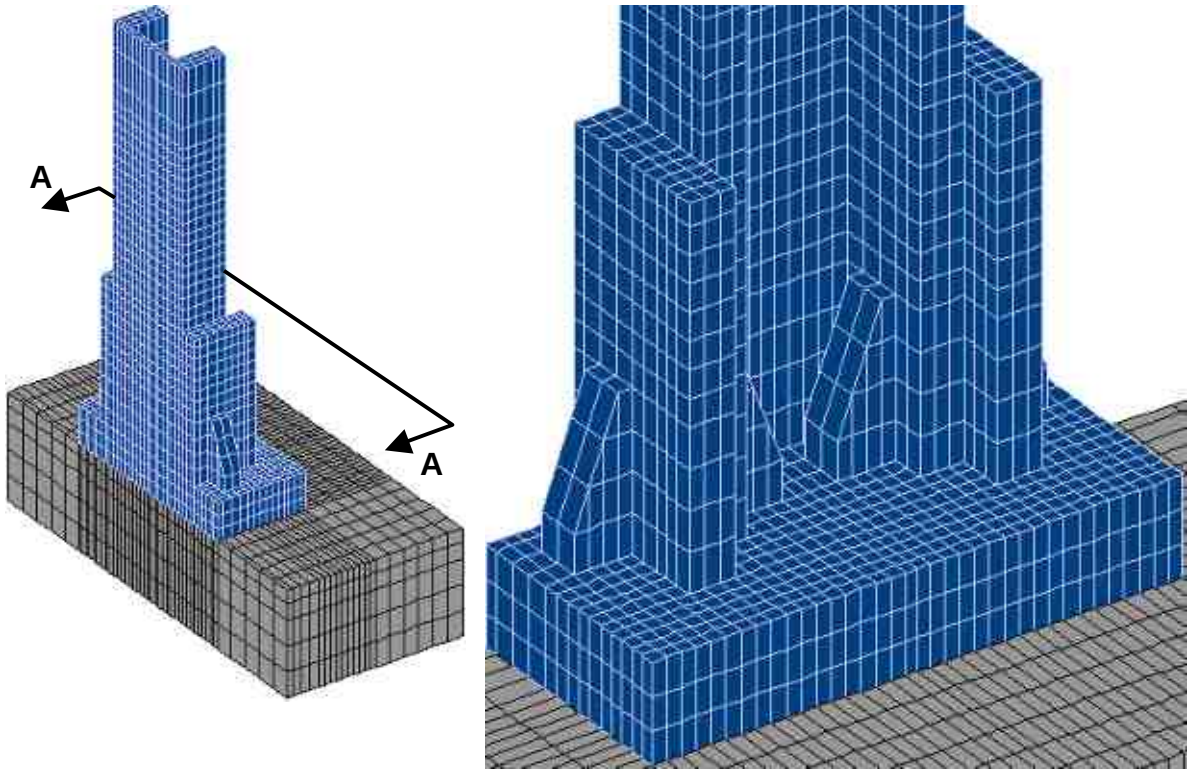

(a) (b)

Figure 4: Finite element model: (a) Typical finite element discretisation of a symmetric half of column-to-foundation subassemblage, and (b) Close-up view of the inner rib plates. Finer mesh is used near the column-to-foundation connection region to capture the stresses in the region.

Results of Pushover Analysis

The horizontal load-drift curves of the four subassemblages are shown in Figure 5. In these curves, the horizontal load H is normalized with the horizontal load H_{pc} required to develop a moment equal nominal plastic moment capacity M_{pc} (= Z_cF_y) in the column, at the end of column-to-foundation connection reinforcement region, given by

$$H_{pc} = \frac{M_{pc}}{(h - t_{bc} - l_c)}, \tag{1}$$

where h is the total height of column subassemblage above the concrete pedestal, t_{bc} the thickness of base plate, and l_c the height of the column-to-foundation connection reinforcement region (Figure 3). The lateral drift of the column-to-foundation connection subassemblage is defined as

$$\delta = \Delta / h, \tag{2}$$

where Δ is the horizontal displacement imposed at the top of the column.

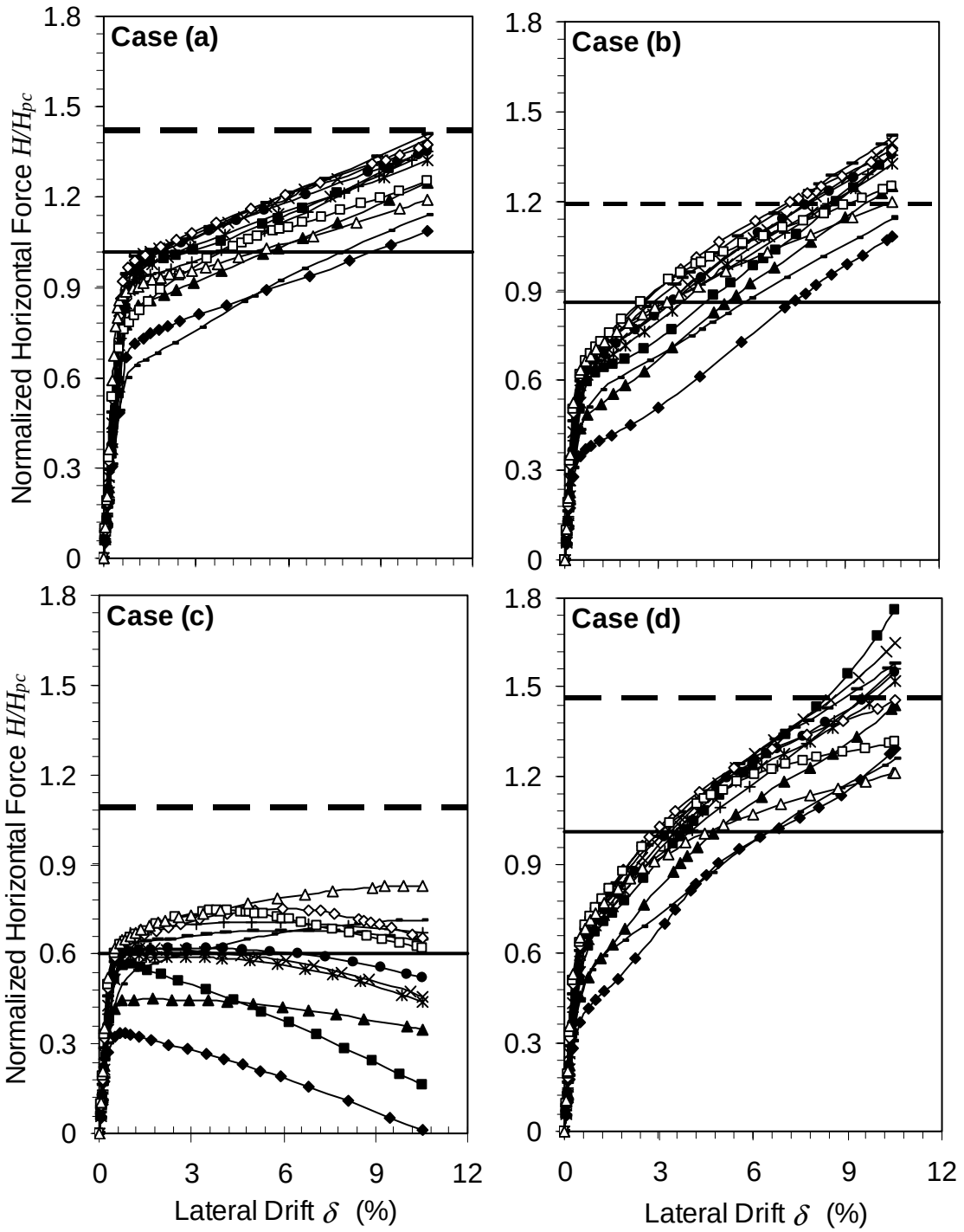

Figure 5: Inelastic response of column-to-foundation connection subassemblage: Normalized horizontal load versus drift curves for four loading cases. The dropping part in case (c) subassemblages is because of the axial force in the column reaching its yield capacity.

For the subassemblages of case (a), i.e., lightly loaded column with large lateral drift, the nonlinear response begins between $0.6H_{pc}$-$0.9H_{pc}$. While, for subassemblages of cases (b), (c) and (d), i.e., heavily loaded columns, the nonlinear response begins between $0.3H_{pc}$-$0.6H_{pc}$. The difference in the starting of the nonlinear response in these cases is because of the initial load – $0.2P_y$ and $0.5P_y$ in cases (a), and (b), (c) and (d) respectively. Thus, the columns of the subassemblages subjected to case (a) loading have larger reserve elastic capacity than those subjected to cases (b), (c) and (d) loadings. In case (c), the lateral load-drift curves drop rapidly after attaining the peak value. While, for case (d), the curves pick load with increasing drift.

For case (c) loading, the initial monotonic pushover load of $0.5P_y$ is applied (along with drift) in addition to the initial gravity load of $0.5P_y$. Thus, for higher steps of the lateral pushover analysis, the axial force on the column approaches the axial force capacity P_y of the column, which is indicated by the dropping part of the horizontal force versus drift curves. On the contrary, in case (d), the axial force on the column is reduced for higher steps of the lateral pushover analysis, resulting in gain of lateral load carrying capacity, which is indicated by the stiffening horizontal force versus drift curves.

In the pushover analyses of the column-to-foundation connection subassemblages, the material property uncertainty factor R_y is taken as 1.0. Thus, for an initial gravity load in columns of $0.2P_y$, the maximum developable moment capacity in columns, according to $\frac{M}{M_{pc}} = \frac{F_u}{F_y}\left[1 - \left\{\left(\frac{F_y}{F_u}\right)\left(\frac{P}{P_y}\right)\right\}^{1/0.7}\right]$ (Arlekar and Murty, 2002), is $1.42M_{pc}$, and for a compressive load of $0.5P_y$, it is $1.19M_{pc}$. Figure 6 shows the *P-M* interaction curve along with the 4% capacity points for the W14×155 column. At 4% horizontal drift, the average moment mobilized in the column are $1.02M_{pc}$, $0.86M_{pc}$, $0.60M_{pc}$, and $1.01M_{pc}$ in the cases (a), (b), (c), and (d), respectively (Table 2). Thus, in general, the actual connection forces exceed those corresponding to the plastic capacity of the column M_{pc} only in cases (a) and (d). The actual axial compressive loads at 4% lateral drifts in cases (a) and (d) are $0.2P_y$ and $0.12P_y$, respectively; these imply full overstrength to column moment capacities of $1.42M_{pc}$ and $1.46M_{pc}$, respectively. Moreover, from Table 3, the average column reserve capacities are 28% and 30% in cases (a) and (d), respectively. The average reserve capacities in cases (b) and (c) are 28% and 40%, respectively.

These unutilized column capacities suggest that the proposed seismic design of column-to-foundation connections may be overestimating the connection design forces. But, if the actual yield strength (R_yF_y) is larger than the nominal yield strength F_y, the additional reserve strength due to this will contribute towards improves performance of the MRF. Further detailed studies are necessary to identify possible reduction in the design forces for column-to-foundation connections, particularly incorporating the flexibility of soil and inelasticity in concrete pedestal and anchor bolts.

SUMMARY AND CONCLUSIONS

The performance of column-to-foundation sub-assemblages subjected to monotonic post-elastic loads has been examined. The column-to-foundation connections are designed according to the capacity design concepts in conjunction with the AISC design procedure for the design of column base plates. A comparison of column moment capacities mobilized with the maximum developable capacities show that there may be some column capacity unutilized, which means that the current design procedure may result in an overestimate of the column-to-foundation design forces. Further studies are needed to validate the proposed procedure (Arlekar and Murty, 2002) and to identify the possible reduction in the design forces.

Table 2: Level of inelasticity mobilized (H/H_{pc}) in column-to-foundation connection subassemblages at 4% drift.

Column Section	H/H_{pc}			
	Case (a) ($0.2P_y$) + Pushover (200mm)	**Case (b) ($0.5P_y$) + Pushover (200mm)**	**Case (c) ($0.5P_y$) + Pushover ($0.5P_y$ and 200mm)**	**Case (d) ($0.5P_y$) + Pushover ($-0.4P_y$ and 200mm)**
W36×300	0.99	0.90	0.75	0.98
W27×178	1.03	0.98	0.75	1.09
W21×147	1.13	1.00	0.73	1.12
W16×100	1.12	0.96	0.67	1.11
W14×730	0.82	0.75	0.63	0.81
W14×455	1.03	0.90	0.70	1.01
W14×257	1.11	0.91	0.62	1.09
W14×176	1.08	0.88	0.59	1.06
W14×61	1.11	0.92	0.60	1.09
W12×336	0.96	0.76	0.44	0.94
W12×210	0.84	0.58	0.25	0.81
W10×112	1.06	0.82	0.46	1.03
Average	**1.02**	**0.86**	**0.60**	**1.01**

Table 3: Comparison of actual and developed column moment capacities at 4% drift.

Case	***Loading***	$\frac{P_{4\%}}{P_y}$	***Capacity Factor at 4% Drift***		***Reserve Capacity at 4% Drift***	
			Actual $\frac{M_{\max}}{M_{pc}}$	***Developed*** $\frac{M^{4\%}}{M_{pc}}$	***Percentage*** $\frac{M_{\max}-M^{4\%}}{M_{\max}}\times 100$	***Factor*** $\frac{M_{\max}}{M^{4\%}}$
(a)	**($0.2P_y$) + Push (200mm)**	0.20	1.42	1.02	28.2	1.39
(b)	**($0.5P_y$) + Push (200mm)**	0.50	1.19	0.86	27.7	1.38
(c)	**($0.5P_y$) + Push ($0.5P_y$ and 200mm)**	0.69	1.01	0.60	40.6	1.68
(d)	**($0.5P_y$) + Push ($-0.4P_y$ and 200mm)**	0.12	1.46	1.01	30.8	1.45

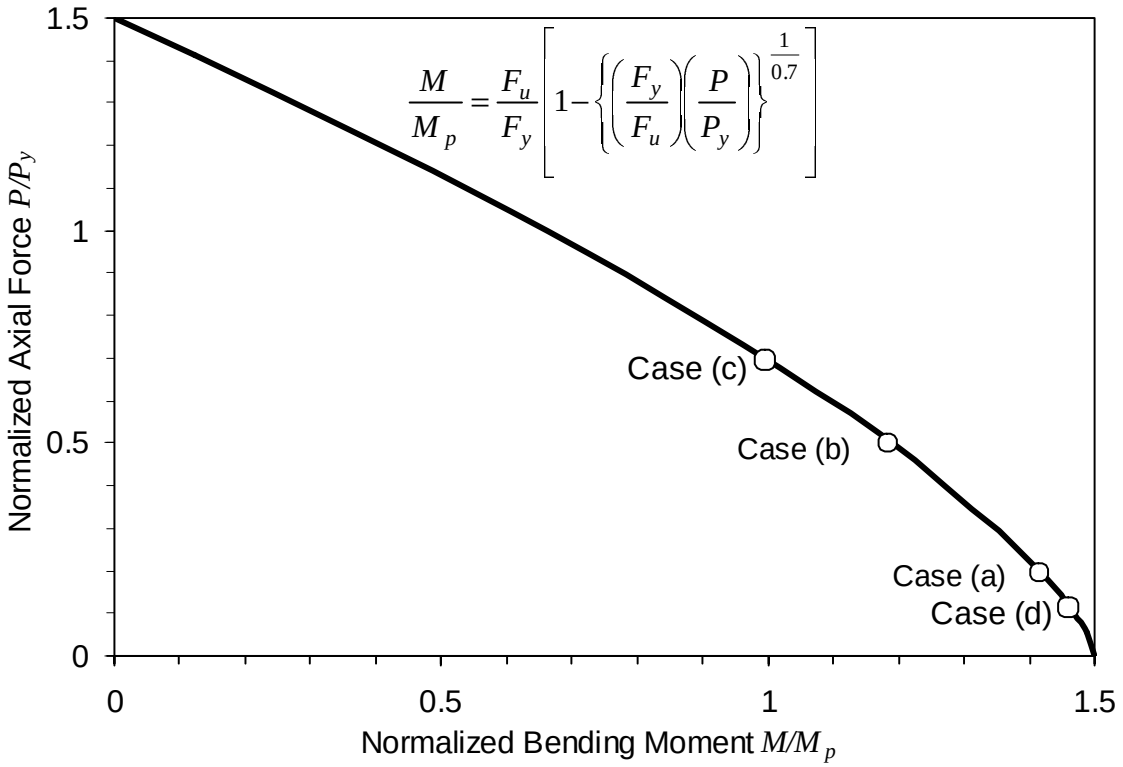

Figure 6: Comparison of four cases for a typical column (W14×155): Column capacities at 4% drift the column-to-foundation connection subassemblage cases considered. The connection design forces for the column-to-foundation with least axial load are the most critical.

REFERENCES

1. AIJ, "Preliminary Reconnaissance Report of the 1995 Hyogoken-Nanbu Earthquake," English Edition, Architectural Institute of Japan, April, 1995.
2. AISC, Manual of Steel Construction Allowable Stress Design – Ninth Edition, American Institute of Steel Construction, Inc., USA, 1989.
3. AISC, Steel Design Guide Series 1 – Column Base Plates, American Institute of Steel Construction, USA, 1990.
4. Arlekar, J. N., "Seismic Design of Strong-Axis Welded Connections in Steel Moment Resisting Frame Buildings," Ph.D. Thesis, Department of Civil Engineering, Indian Institute of Technology Kanpur, India, 2002.
5. Arlekar, J. N., and Murty, C.V.R., "P-V-M Interaction Curves for Seismic Design of Column Base Connections," Engineering Journal, 3rd Quarter, pp. 154-165, American Institute of Steel Construction, USA, 2002.
6. Bertero, V. V., Anderson, J. C., and Krawinkler, H., "Performance of Steel Building Structures during the Northridge Earthquake," Report No. UCB/EERC-94/09, Earthquake Engineering Research Center, College of Engineering, University of California at Berkeley, 1994.
7. HKS, ABAQUS/Standard User's Manual, Hibbitt, Karlsson & Sorensen, Inc., RI, USA, 1998.